Boletim da Sociedade Astronômica Brasileira, **35**, no. 1, 199-203

Polarimetric results of the SPARC4 commissioning

A. C. Mattiuci[1], E. Martioli[2], C. V. Rodrigues[1], J. C. N. Campagnolo[3], W. Schlindwein[1], F. Falkenberg[1], & D. Bernardes[1]

[1] Instituto Nacional de Pesquisas Espaciais, São José dos Campos, SP, Brazil e-mail: ana.figueiredo@inpe.br
[2] Laboratório Nacional de Astrofísica, Itajubá, MG, Brazil
[3] Centro Federal de Educação Tecnológica Celso Suckow da Fonseca, Rio de Janeiro, RJ, Brazil

Abstract. The Simultaneous Polarimeter And Rapid Camera in four bands (SPARC4) is an imager capable of simultaneously observing four photometric bands (g, r, i, z) in both photometric and polarimetric modes. SPARC4 operates at the 1.6 m Perkin-Elmer telescope at the Observatório do Pico dos Dias (OPD). The instrument is a project led by the Instituto Nacional de Pesquisas Espaciais (INPE) in partnership with the Laboratório Nacional de Astrofísica (LNA). The first commissioning run took place in November 2022. In this run, we observed the polarimetric standard star NGC 2024 1 and obtained a good result, which demonstrates that the instrument's polarimetric mode is working correctly. Since then, other polarimetric standard stars have been observed on the commissioning and science verification SPARC4 runs, with half- and quarter-wave plates. We present the analysis of these polarimetric data, discuss the results and compare our results with the literature.

Resumo. A SPARC4 (do inglês *Simultaneous Polarimeter And Rapid Camera in 4 bands*) é um imageador capaz de observar simultaneamente em quatro bandas (g, r, i, z) nos modos fotométricos e polarimétricos. A SPARC4 atua no telescópio Perkin-Elmer de 1.6 m localizado no Observatório do Pico dos Dias (OPD). O instrumento é um projeto liderado pelo Instituto Nacional de Pesquisas Espaciais (INPE) em parceria com o Laboratório Nacional de Astrofísica (LNA). A primeira missão de comissionamento ocorreu em novembro de 2022. Nesta missão, foi observada a padrão polarimétrica NGC 2024 1 e obtivemos um bom resultado, que demonstra que o modo polarimétrico do instrumento está funcionando corretamente. Desde então, outras padrões polarimétricas tem sido observadas nas missões da SPARC4 de comissionamento e verificação de ciência, com lâminas de meia onda e quarto de onda. Nós iremos apresentar a análise desses dados polarimétricos, discutir os resultados e comparar nosso resultados com a literatura.

Keywords. Instrumentation: photometers – Instrumentation: polarimeters – Methods: observational – Techniques: polarimetric – Standards

1. Introduction

The Simultaneous Polarimeter And Rapid Camera in four bands (SPARC4) is capable of observing in the photometric (Schlindwein et al. 2024) and polarimetric (this work) modes with a time resolution of 1 s or better in four bands (g, r, i, z), with a simultaneously observing field of view of 5.8 × 5.8 arcmin^2. Many scientific cases can benefit from the SPARC4 polarimetric mode, such as interacting binaries, exoplanets, circumstellar envelopes, star-forming regions, blazars, and open clusters (Rodrigues et al. 2012, 2024). In the first half of 2024, SPARC4 will be available to astronomic community.

The SPARC4 commissioning runs started in November 2022 and continued throughout the year 2023, spanning the months of February, April, May, June, July, August, September and November. Additionally, scientific verifications were carried out in June and July. Taking into consideration the polarimetric function of the instrument, some objectives of the runs are to verify instrument performance in polarimetry; to compare polarization values with literature; to test instrument and pipeline stability for polarimetry; to assess the instrumental efficiency and polarization, and to measure the position of the fast axis of the waveplates.

The polarimetric module of SPARC4 is composed of a rotating half- or quarter-wave plate retarder ($\lambda/2$ or $\lambda/4$ respectively) and a Savart prism, responsible for dividing the flux of the object into two components, the ordinary flux ($F_o(\phi)$) and the extraordinary flux ($F_e(\phi)$). The waveplate system has 16 rotating positions present, each separated by 22.5 degrees. (Rodrigues et al. 2012).

The SPARC4 pipeline is an open source data reduction software based on the ASTROnomical POlarimetry and Photometry Pipeline (ASTROPOP, Campagnolo 2018, Campagnolo et al. 2024). This code is written in Python and uses the standard Astropy[1] 5 FITS Image HDU class. ASTROPOP can perform image preprocessing, source detection, photometric and polarimetric reduction, and astrometric and photometric calibration. The pipeline is planned to be the default mode of SPARC4 data reduction. As part of the pipeline's development, a separate set of Python notebooks, created using ASTROPOP and other tools, was manually prepared to extensively test reduction techniques. The results presented here are derived from these notebooks, which form the foundation for the automated reduction in the SPARC4 pipeline, to be provided to users along with regular scientific operations.

This contribution is organized as follows. In Sec. 2, we present the details of seven polarimetric observations from SPARC4. The description of data reduction using ASTROPOP is in Sec. 4. Section 3 shows our main results and a comparison of the literature. Our conclusions and future work are given in Sec. 5. We also provide more information about the observations in the Appendix A.

2. Polarimetric standards observations

The commissioning runs of SPARC4 included observations of polarimetric standard stars, polarized or not. A polarimetric measurement consists of a sequence of images obtained in different

[1] https://astropy.org

Table 1. Summary of observations.

Object (Retarder)	Date	Band	t_{exp} (s)	# Exp.
NGC 2024 1	2022 Nov 15	g	60.00	48
(λ/2)		r	30.00	96
		i	20.00	144
		z	15.00	192
Vela1 95	2023 Jun 09	g	30.00	16
(λ/2)		r	3.00	160
		i	3.00	160
		z	10.00	48
HD 111579	2023 May 02	g	5.00	16
(λ/2)		r	1.00	80
		i	1.50	48
		z	2.50	32
	2023 May 03	g	1.00	16
		r	0.30	16
		i	0.40	16
		z	0.50	16
	2023 Jun 04	g	6.00	16
		r	1.00	48
		i	1.25	48
		z	1.25	48
	2023 Jun 06	g	6.00	16
		r	1.50	64
		i	3.00	32
		z	3.00	32
Hilt 781	2023 Jun 04	g	20.00	16
(λ/2)		r	2.00	160
		i	2.00	160
		z	4.00	80
HD 111579	2023 May 02	g	5.00	16
(λ/4)		r	0.50	64
		i	1.00	48
		z	2.50	32
	2023 May 03	g	1.00	16
		r	0.30	16
		i	0.40	16
		z	0.50	16
	2023 Jun 04	g	6.00	16
		r	1.00	48
		i	1.25	48
		z	1.25	48
	2023 Jun 06	g	6.00	16
		r	1.50	64
		i	3.00	32
		z	3.00	32

waveplate positions. The observations were performed with λ/2 or λ/4 and the analyzer. For each waveplate position, we collected one or more images, depending on the band and exposure time.

3. Results

The first polarimetric standard observed by SPARC4 was NGC 2024 1, a B-type star (V = 12.17) and a member of a young cluster (Broos et al. 2013) within the Flame Nebula, which is polarized by interstellar dust. Since then, SPARC4 has already observed ten other polarimetric standards, the majority with two or more observations. In the Tab. 1 we present the details of seven SPARC4 polarimetric observations, the results of which are given in Sec. 3. In the Tab. 5, we present all standard polarimetric observations made with SPARC4.

4. Data reduction

All reductions were performed using ASTROPOP. The cosmic ray extraction uses the ASTROSCRAPPY[2] package, and the bias and flat-field corrections use built-in functions similar to the IRAF tasks *imarith* and *imcombine*. Then, we calculate the shifts between the images to create the stack image. With this image, the sources are detected using the function *starfind* which is implemented with the SEP (Barbary 2016) and DAOPHOT algorithms (Stetson 1987).

Since we are working with polarimetric frames, where we have the ordinary and extraordinary beams, ASTROPOP matches the pairs before performing the aperture photometry. In this step, ASTROPOP allows us to obtain the aperture photometry for all the pairs identified using a range of aperture radii, calculated proportionally to the full width at half maximum (FWHM).

To obtain the Stokes parameters from the ordinary and extraordinary fluxes ($F_o(\phi)$ and $F_e(\phi)$), ASTROPOP uses the Stokes Least Squares (SLS) method with the attribute COMPUTE, in which we have to pass the waveplate position angle in degrees (ϕ), $F_o(\phi)$ and $F_e(\phi)$. This method calculates the normalized flux difference between the fluxes ($Z(\phi)$) for each ϕ (Rodrigues et al. 1998).

$$Z(\phi) = \frac{F_o(\phi) - F_e(\phi) \cdot k}{F_o(\phi) + F_e(\phi) \cdot k}, \quad (1)$$

where k is a normalization factor (for λ/2, $k = \frac{\sum F_o(\phi)}{\sum F_e(\phi)}$) (Magalhaes et al. 1984). $Z(\phi)$ is a function of the Stokes parameters (Q, U, and V), which, in turn, is related to the linear polarization (P) and the polarization angle (PA).

For λ/2 waveplate:

$$Z(\phi) = Q \cdot cos\,4\phi + U \cdot sin\,4\phi, \quad (2)$$

and for λ/4 waveplate:

$$Z(\phi) = Q \cdot cos^2\,2\phi + U \cdot sin\,2\phi\,cos2\phi - V \cdot sin\,2\phi. \quad (3)$$

Polarimetric products are the values of $q = \frac{Q}{I}$, $u = \frac{U}{I}$, $v = \frac{V}{I}$, P, PA with their uncertainties and the theoretical expected error based on the signal-to-noise ratio (SNR) of the fluxes (*theor_sigma*).

For λ/2 waveplate:

$$\sigma_P = \sigma_Q = \sigma_U = \frac{\sqrt{2}}{SNR}. \quad (4)$$

For λ/4 waveplate:

$$\sigma_Q = \frac{1}{\sqrt{0.396} \cdot SNR}; \quad \sigma_U = \frac{1}{\sqrt{0.1464} \cdot SNR};$$

$$\sigma_V = \frac{1}{\sqrt{0.4571} \cdot SNR}; \quad \sigma_P = \frac{\sqrt{Q^2 \cdot \sigma_Q^2 + U^2 \cdot \sigma_U^2}}{P}. \quad (5)$$

In addition to the products, we have a $Z(\phi)$ versus ϕ diagram, Fig. 1 is an example. In this figure, we show the $Z(\phi)$ versus waveplate position angle diagram for NGC 2024 1 in the four bands (g, r, i, z) for the λ/2 retarder plate. The black dots at the top show $Z(\phi)$ with the retarder plate position, and the red curve

[2] https://github.com/astropy/astroscrappy

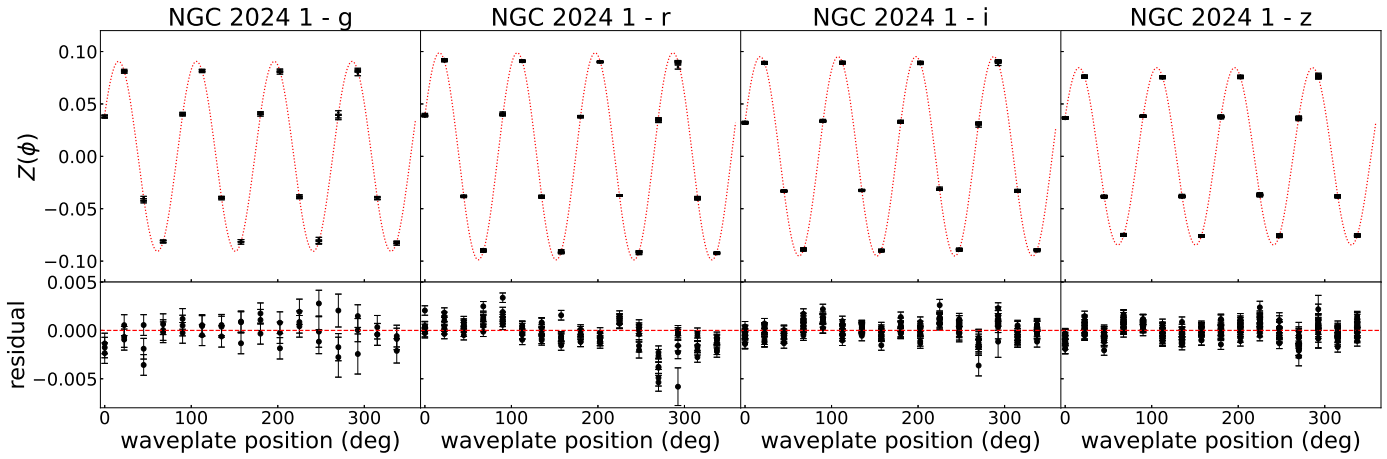

Figure 1. $Z(\phi)$ versus ϕ for NGC 2024 1 in the four bands (g, r, i, z) with a $\lambda/2$ retarder plate.

Table 2. Comparison between ASTROPOP pipeline, ASTROPOP notebook, and IRAF for HD 111579 in the g-band with a half-wave retarder plate.

Reduction	q (%)	u (%)	P (%)	PA (deg)
Pipeline	-2.32 ± 0.08	-5.73 ± 0.09	6.18 ± 0.09	124 ± 0.40
Notebooks	-2.34 ± 0.08	-5.72 ± 0.08	6.18 ± 0.08	124 ± 0.40
IRAF	-2.33 ± 0.08	-5.76 ± 0.08	6.21 ± 0.08	124 ± 0.37

Table 3. Median and median absolute deviation (MAD) for the polarization (P), and the median for the polarization error (σ_P) for HD 111579 with half-wave retarder plate.

band	Median (P) (%)	MAD (P) (%)	Median (σ_P) (%)
g	6.1587	0.0214	0.0318
r	6.3470	0.0247	0.0270
i	5.8525	0.0123	0.0309
z	4.9580	0.0035	0.0471

is a model of q and u from 0 to 360°. Below, the dots are the residuals of the model relative to the observations, and the red line indicates the zero level.

In this section, we present some results on SPARC4 polarimetry. We made comparisons between our results obtained with ASTROPOP and IRAF and between our results and the literature for $\lambda/2$ retarder plate. Finally, we present a preliminary result for $\lambda/4$ retarder plate. For this contribution, we analyze seven SPARC4 observations (see Tab. 1), four of which are from the same object (HD 111579) observed on different dates. We still have 28 observation data sets to finish the analysis, so this work is the beginning of the SPARC4 characterization.

In Tab. 2, we bring a result of a standard polarimetric, HD 111579, a B-type star (V = 9.12) in the g-band, with a retarder plate $\lambda/2$. We compare the polarimetric reduction between the IRAF, ASTROPOP notebooks, and ASTROPOP pipeline. We used the same aperture photometry. This result shows the stability between ASTROPOP notebooks and ASTROPOP pipeline.

In Fig. 2, we see P for $\lambda/2$ for the same object (HD111579) observed on four different dates. In general, P is higher in the r-band and lower in the z-band. This peak in the visual bands is expected according to the work of Serkowski et al. (1975) on the dependence of P with wavelength. In Tab. 3, we see the median and median absolute deviation (MAD) for P and the median for the polarization error (σ_P). The MAD(P) is lower than the median(σ_P), that is, our measurements are stable.

We chose three objects to compare with the literature, NGC 2024 1, Hilt 781, and Vela1 95. Polarimetry for these objects was also published by Fossati et al. (2007) and Cikota (2017). Fossati et al. (2007) analyzed polarimetric standards to calibrate the FOcal Reducer and the low dispersion Spectrograph (FORS1) with imaging polarimetric mode (IPOL) and spectropolarimetric mode (PMOS) in the Bessel B, V, R, and I bands. Ten years later, Cikota (2017) made similar work for FORS2 with PMOS mode.

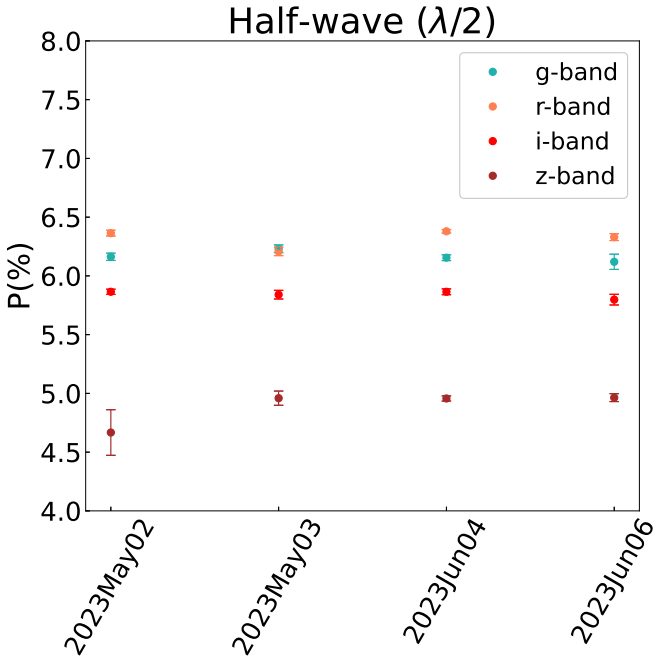

Figure 2. The linear polarization of HD 111579 measured in four nights using the half-wave retarder plate.

In Fig. 3, we compare our results with Fossati et al. (2007) and Cikota (2017). Looking only at our result (black dots), we can analyze them again with the Serkowski et al. (1975) studies. There is a peak in the r band for NGC 2024 1 and Vela1 95. In Hilt. 781 this result is not clear. Still, taking into account the

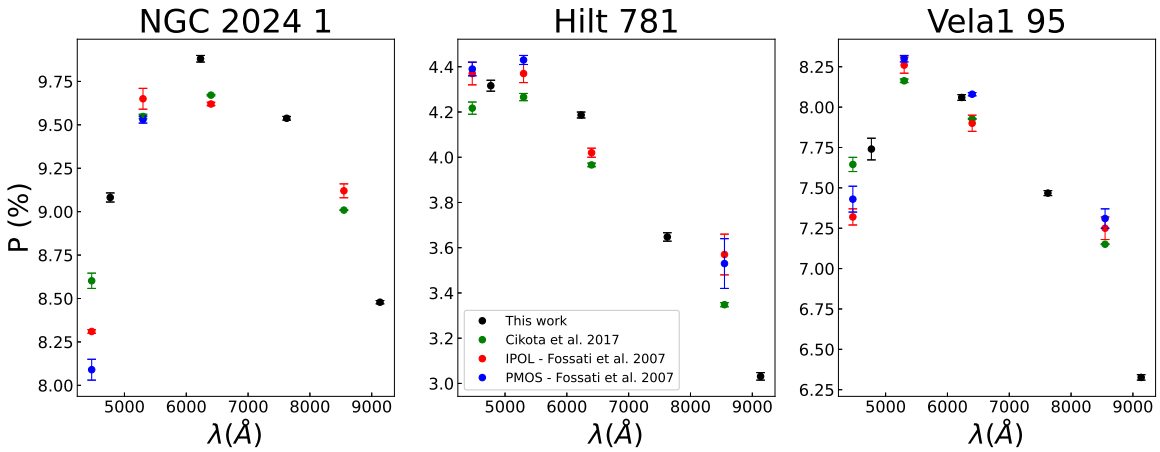

Figure 3. Comparison with the literature for NGC 2024 1, Hilt 781, and Vela1 95.

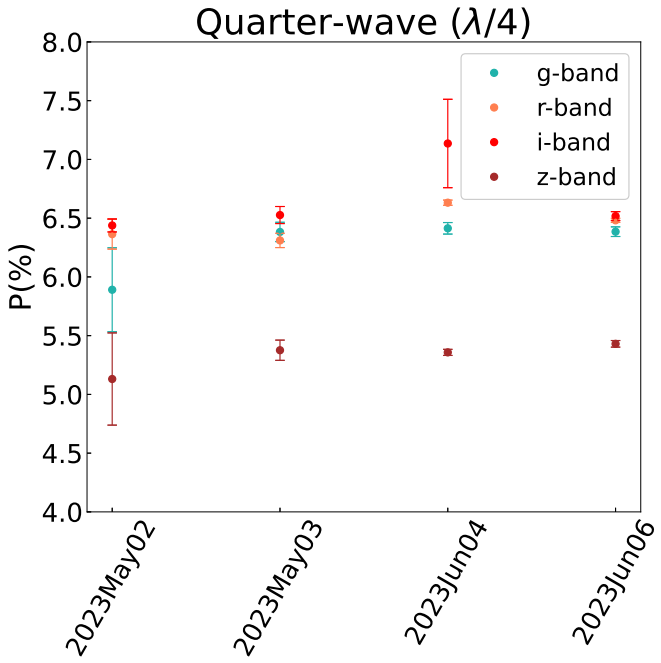

Figure 4. The linear polarization of HD 111579 measured in four nights using the quarter-wave retarder plate.

Table 4. Median and median absolute deviation (MAD) for the polarization (P), and the median for the polarization error (σ_P) for HD 111579 with quarter-wave retarder plate.

band	Median (P) (%)	MAD (P) (%)	Median (σ_P) (%)
g	6.3838	0.0155	0.0656
r	6.4227	0.0855	0.0415
i	6.5221	0.0443	0.0639
z	4.3667	0.0364	0.0571

difference between the bands and the observations mode, all our results are consistent with the literature.

Finally, we present an introductory analysis with the $\lambda/4$ retarder plate. In Fig. 4 we see P values for HD 111579, in the four bands (g, r, i, z) observed on four different dates, with the $\lambda/4$ retarder plate.

In Tab. 4 we have the median and MAD for P, and the median for σ_P. The P medians with $\lambda/4$ are higher than the P medians with $\lambda/2$, except in the z-band. For the r-band, the MAD(P) is higher than the median(σ_P), so this result is not stable. In general, these values are not ideal, because, with $\lambda/4$, we have another factor that implies in the result, the zero degree of the waveplate.

The zero degree will be unique in SPARC4, however, variations may occur due to the band and waveplate retardance. These values are not defined yet. In Fig. 5, we present a preliminary result for the zero position of the waveplate calculated for HD 111579, also on four different dates. The dots are the zero value, the continuous lines are the median, and the dashed lines are the MAD of the zero values for each band. In bands g, i, and z, we have a small variation in the zero values, lower than 10 *deg* considering the errors, but this variation doubles for the r-band. Therefore, we have to continue this study, including other objects on the same and different dates, and consider everything that may have changed the zero degree in the instrument.

5. Conclusion and Perspectives

The polarimetric mode of SPARC4 presents promising results in terms of both efficiency and polarimetry quality. Although full characterization is still ongoing, the instrument is relatively stable and the polarimetric mode is fully operational for scientific use, exhibiting strong potential for measuring linear and circular polarization in both field and time series observations. Also, there is a functional pipeline to run the automatic reduction of polarimetric data.

Our next steps are: to implement an automatic reduction of polarimetric standards, write a calibration protocol to be followed by all programs and monitor instrumental calibration over time, measure the angle between SPARC4 polarimetry and North orientation (e.g., from asteroids), and measure performance of polarimetric mode for both photometric and polarimetric time series.

Acknowledgements. SPARC4 team thanks FINEP (0/1016/0076/00) and the Brazilian Space Agency (AEB), CNPq (CVR:310930/2021-9) for the grant in the process. A.C.M thanks to CNPq (310930/2021-9), INPE for the opportunity and supervision, and OPD-LNA for the observations. C.V.R. thanks CNPq (310930/2021-9). E.M. acknowledges funding from FAPEMIG (APQ-02493-22) and CNPq for a research productivity grant number 309829/2022-4. W.S. thanks CNPq (300343/2022-1). D.V.B. thanks CAPES (88887.513623/2020-00).

Table 5. Polarimetric Standard observations.

Star ID	V (mag)	Observed dates	Ref.
NGC 2024 1	12.17	2022 Nov 15; 2023 Nov 5 & 6	Broos et al. 2013
HD 111579	9.12	2023 May 2 & 3; Jun 04, 06 & 13; Jul 07 & 11	Stephenson & Sanduleak 1971
HD 126593	8.65	2023 May 3 & 5; Jun 1 & 5	Stephenson & Sanduleak 1971
HD 298383	9.75	2023 May 04; Jun 05	Bok et al. 1972
Hilt 652	10.61	2023 May 02 & 05; Jun 01 & 07; Sep 20	Stephenson & Sanduleak 1971
Vela1 95	12.12	2023 May 04; Jun 09	Vieira et al. 2003
Hilt 781	10.71	2023 Jun 04 & 11; Aug 30; Sep 20 & 21	Stephenson & Sanduleak 1971
HD 155528	9.60	2023 Jul 06 & 09	Bingham et al. 1976
HD 316232	10.17	2023 Aug 31; Sep 21	Stephenson & Sanduleak 1971
Hilt 715	9.56	2023 Aug 31; Sep 21	Stephenson & Sanduleak 1971
Hilt 785	10.20	2023 Sep 28	Jaschek & Egret 1982

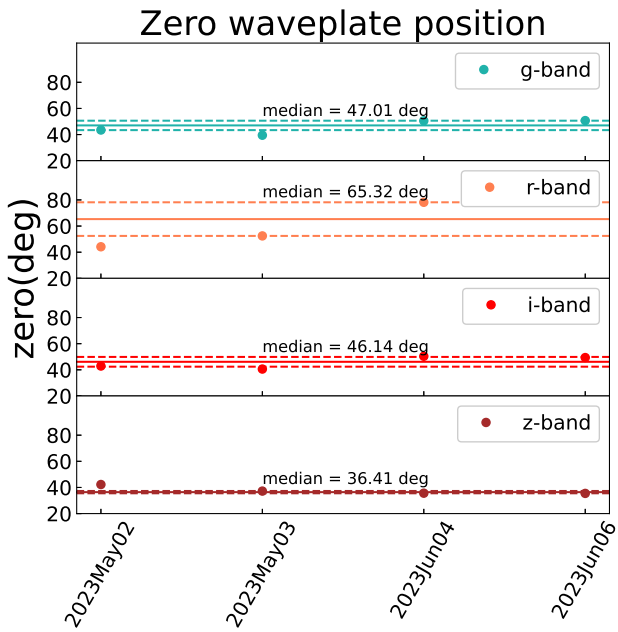

Figure 5. Zero waveplate position calculated for HD 111579 on four different dates.

Apêndice A: Summary of observations

In this appendix we bring the summary of the observations all objects already observed by SPARC4. Table 5 has the magnitude of the objects, the observed dates and the references.

References

Barbary, K. 2016, The Journal of Open Source Software, 1, 58
Bingham, R. G., McMullan, D., Pallister, W. S., et al. 1976, Nature, 259, 463
Bok, B. J., Bok, P. F., & Miller, E. W. 1972, AJ, 77, 733
Broos, P. S., Getman, K. V., Povich, M. S., et al. 2013, ApJS, 209, 32
Campagnolo, J. C. N. 2018, Astrophysics Source Code Library. ascl:1805.024
Campagnolo J. C. N., et al., 2024, BoSAB, this volume
Cikota, A. 2017, ESO Calibration Workshop: The Second Generation VLT Instruments and Friends, 7
Fossati, L., Bagnulo, S., Mason, E., et al. 2007, The Future of Photometric, Spectrophotometric and Polarimetric Standardization, 364, 503
Jaschek, M. & Egret, D. 1982, Be Stars, 98, 261
Magalhaes, A. M., Benedetti, E., & Roland, E. H. 1984, PASP, 96, 383
Rodrigues, C. V., Cieslinski, D., & Steiner, J. E. 1998, A&A, 335, 979
Rodrigues, C. V., Taylor, K., Jablonski, F. J., et al. 2012, Proc. SPIE, 8446, 844626
Rodrigues, C. V., et al., 2024, BoSAB, this volume
Schlindwein, W., et al., 2024, BoSAB, this volume
Serkowski, K., Mathewson, D. S., & Ford, V. L. 1975, ApJ, 196, 261
Stephenson, C. B. & Sanduleak, N. 1971, Publications of the Warner & Swasey Observatory, 1, 1
Stetson, P. B. 1987, PASP, 99, 191
Vieira, S. L. A., Corradi, W. J. B., Alencar, S. H. P., et al. 2003, AJ, 126, 2971